

SCIENTIFIC REPORTS



OPEN

Silica precipitation potentially controls earthquake recurrence in seismogenic zones

Hanae Saishu^{1,2}, Atsushi Okamoto³  & Makoto Otsubo²

Silica precipitation is assumed to play a significant role in post-earthquake recovery of the mechanical and hydrological properties of seismogenic zones. However, the relationship between the widespread quartz veins around seismogenic zones and earthquake recurrence is poorly understood. Here we propose a novel model of quartz vein formation associated with fluid advection from host rocks and silica precipitation in a crack, in order to quantify the timescale of crack sealing. When applied to sets of extensional quartz veins around the Nobeoka Thrust of SW Japan, an ancient seismogenic splay fault, our model indicates that a fluid pressure drop of 10–25 MPa facilitates the formation of typical extensional quartz veins over a period of 6.6×10^0 – 5.6×10^1 years, and that 89%–100% of porosity is recovered within $\sim 3 \times 10^2$ years. The former and latter sealing timescales correspond to the extensional stress period ($\sim 3 \times 10^1$ years) and the recurrence interval of megathrust earthquakes in the Nankai Trough ($\sim 3 \times 10^2$ years), respectively. We therefore suggest that silica precipitation in the accretionary wedge controls the recurrence interval of large earthquakes in subduction zones.

Earthquake recurrence intervals are commonly used to predict the timescales of future earthquakes^{1–3}. However, many unresolved factors add ambiguity to any discussion of the timescales of seismic cycles, including which parameters control earthquake triggering and the timescales required to change crustal conditions from aseismic to seismic. It has been suggested that the distribution of high pore pressures within the seismogenic zone controls earthquake occurrence, as inferred from a combination of seismic data, the porosity of *in situ* rocks, and numerical simulations^{4–7}. The interseismic period related to the cycling of fluid pressure has been explained by changes in tectonic stress and fault strength⁸. In particular, the buildup and release of pore fluid pressure during a seismic cycle promote temporal changes in fault strength. The dissolution and precipitation of minerals play an important role in closing dilatational fractures generated during the co-seismic period and reducing the porosity of rocks⁹. However, the evolution of relevant hydrological properties (e.g., pore fluid pressure, porosity, and permeability) related to water–rock interaction during the interseismic period is poorly understood.

Silica is a dominant component of crustal rocks, and widespread quartz veins in subduction zones at seismogenic depths are taken as proof of significant fluid flow and silica precipitation^{10–12}. Silica–water interaction may play a crucial role in a wide range of seismic phenomena; e.g., the rapid precipitation of large amounts of silica due to a large pressure drop in response to an earthquake^{11,13}, fault weakening by silica gel formation on fault surfaces^{14,15}, and pressure solution and diffusion of silica that occur in relation to slow slip earthquakes^{12,16}. In particular, silica precipitation effectively seals cracks and faults, and could therefore significantly influence the buildup of fluid pressure during the interseismic period^{8,17,18}. However, no studies have quantitatively discussed the timescales of quartz vein formation and earthquake recurrence intervals within subduction zones.

Here we propose a novel kinetic model of quartz vein formation that allows us to estimate the sealing times of isolated cracks based on pore-fluid pressure drop within the crack, advective flow of silica-rich fluids from the peripheral host rock, and quartz crystal growth in the seismic zone. Our model quantifies the relationship between the recurrence intervals of earthquakes and the sealing timescales of quartz-filled extensional cracks around the Nobeoka Thrust, southeastern Japan, a typical seismogenic megasplay fault in an ancient subduction zone.

¹Renewable Energy Research Center, National Institute of Advanced Industrial Science and Technology (AIST), 2-2-9 Machiikedai, Koriyama, Fukushima, 963-0298, Japan. ²Geological Survey of Japan, National Institute of Advanced Industrial Science and Technology (AIST), Tsukuba Central 7, 1-1-1 Higashi, Tsukuba, Ibaraki, 305-8567, Japan. ³Graduate School of Environmental Studies, Tohoku University, 6-6-20 Aramaki-Aza-Aoba, Aoba-ku, Sendai, Miyagi, 980-8579, Japan. Atsushi Okamoto and Makoto Otsubo contributed equally to this work. Correspondence and requests for materials should be addressed to H.S. (email: saishu.h@aist.go.jp)

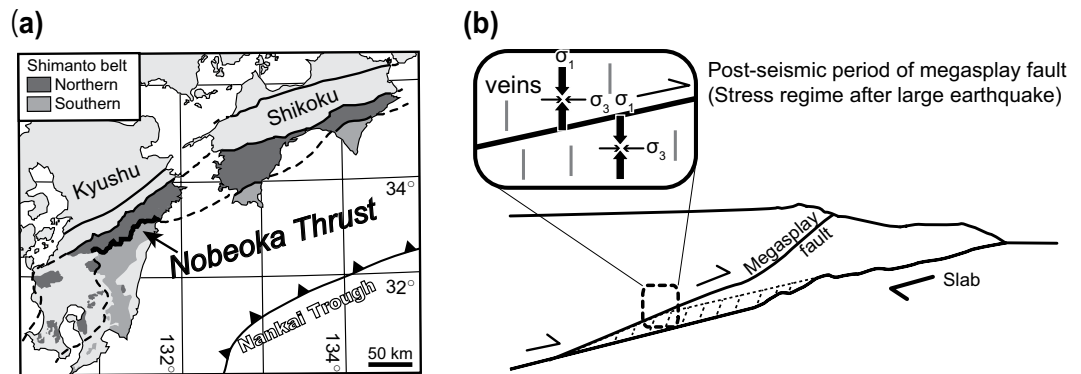


Figure 1. Geological conditions and the formation of extensional veins associated with thrust. **(a)** Geological setting of the Nobeoka Thrust, southwest Japan (modified after ref.⁵²). **(b)** Schematic model of spatial change of stress regimes at post-earthquakes and formation of extension cracks along the subduction zone (modified after ref.²¹). The map **(a)** was created by using Adobe Illustrator⁵³ version CS6 software.

Geological setting and occurrence of extensional quartz veins

The Nobeoka Thrust is a major fault that bounds the northern and southern Shimanto belts of Kyushu, southwestern Japan¹⁹ (Fig. 1a), traceable for >800 km in the Cretaceous–Neogene Shimanto Belt accretionary complex parallel to the modern Nankai Trough¹⁹. The thrust is considered a fossilized megasplay fault due to the presence of pseudotachylite in its hanging wall damage zone²⁰ and its paleotemperatures¹⁹. Its total estimated displacement of ~8.6–14.4 km, based on a 70 °C temperature difference between the hanging wall and footwall, is comparable to the deeper part of the modern megasplay fault in the Nankai Trough^{19,21}.

The veins around the Nobeoka Thrust are classified into three types: extensional crack-filling veins (mode I cracks), fault-filling veins, and post-mélange veins^{19,21–23}. The extensional crack-filling veins, which cut phyllitic shale, mélangé, cataclasite, and composite planer fabrics, are abundant in both the hanging wall and footwall of the Nobeoka Thrust²¹. The stress inversion reveals that the extensional quartz veins formed under a normal faulting type stress regime, with the orientation of the minimum principal stress (σ_3) axis being almost horizontal and trending roughly NNW–SSE in both the hanging wall and footwall²¹ (Fig. 1b). The negative stress of the reverse faulting type stress regime, combined with the σ_3 axis subparallel to the slip direction of the Nobeoka Thrust (top to the SSE)^{21,24}, indicates that the normal faulting type stress regime at the time of fracture opening was secondary stress generated by slip of the Nobeoka Thrust²¹. The temporal stress changes are similar to those of Mw 9.0 2011 Tohoku-Oki earthquake²⁵ and to large trench-type earthquakes along the décollement²⁶. The microstructural features of syntectonic mineral veins have been interpreted as evidence of temporal fluctuations in fluid pressure during repeated earthquake cycles within a seismogenic megasplay fault in an ancient subduction zone²². The extensional veins are consistent with multiple episodes of slip on the Nobeoka Thrust. Analyses of fluid inclusions hosted by rocks of the Shimanto belt in Kyushu reveal that the fluid salinity is similar to or lower than that of seawater²⁷. Geochemical and mineralogical analyses suggest that extensional veins around the Nobeoka Thrust formed from relatively oxidized, locally derived pore fluids with neutral pH²². Analyses of vitrinite reflectance and fluid inclusions reveal that vein formation occurs under both high P – T conditions (260–340 °C, 235–250 MPa) and low P – T conditions (140–250 °C and 150–190 MPa) in the hanging wall and footwall of the Nobeoka Thrust^{19,28,29}. The difference in temperature across the fault was generated by activation of the Nobeoka Thrust as an out-of-sequence-thrust or megasplay fault¹⁹. The normalized pore fluid pressure ratio, the lower bound of the maximum fluid pressure level³⁰, is ~0.95 for a tensile strength of 10 MPa²¹. This stress condition means that the tensile overpressure exceeds σ_3 during the period of vein formation. The formation of high-angle extensional fractures occurs only when tensile overpressure $P_f > \sigma_3$ is attained³¹.

Great earthquakes along the Nankai Trough occurred at intervals of 9×10^1 – 3×10^2 years in the period covered by historical records (684–1946 A.D.)². The high pore pressures were expected to be close to lithostatic pressure along the mega-splay fault of the Nankai Trough⁷. However, there is no consensus on the recurrence intervals of earthquakes on splay/megasplay faults around the Nobeoka Thrust or those of megathrust earthquakes along the Nankai Trough. If we treat the postseismic period (i.e. the period under the secondary stress regime) as having effectively zero aftershock activity after roughly one-tenth of the recurrence interval (as inferred from compiled data and numerical estimates of mainshock recurrence times, and observed and predicted aftershock sequence durations¹), the timescale required to open extensional cracks in the Shimanto accretionary wedge is 9×10^0 – 3×10^1 years.

We observed discrete extensional veins in the hanging wall of the Nobeoka Thrust, filled mainly with quartz and lesser calcite. The aperture widths (w_v) and lengths (l_v) of quartz veins were estimated from eight thin sections (48×22 mm) and field measurements, respectively; both measurements are log-normally distributed, with $w_v = 1.3 \times 10^1$ – 3.4×10^2 μm (geometric mean 5.2×10^1 μm ; Fig. 2a) and $l_v = 1.9 \times 10^0$ – 5.0×10^1 cm (geometric mean 7.4×10^0 cm), with a few veins being longer than 5.0×10^1 cm (Fig. 2b). The vein quartz grew on quartz grain surfaces in vein walls (Figs. 2c,d), and there is no evidence of repeated crack–seal events (i.e. inclusion bands³²).

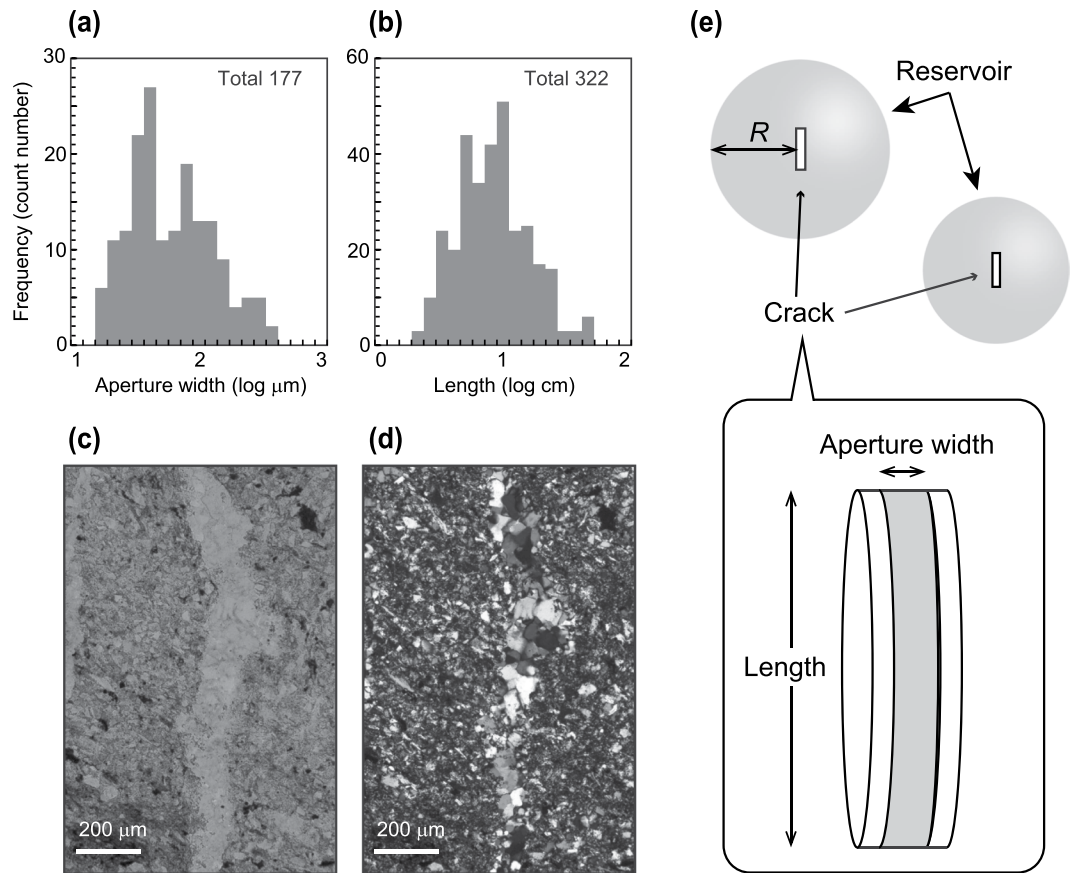


Figure 2. Photos and schematic image of extensional quartz veins observed along the Nobeoka Thrust. The log-size histogram of quartz veins of aperture width measured by using the thin section samples of quartz veins (a), and length measured at the outcrop of the Nobeoka Thrust (b). The photographs of (c) open-nichol and (d) cross nichol of a thin section of quartz veins around the Nobeoka Thrust. (e) Schematic of a crack in a reservoir that formed via advection and kinetic reaction (Supplementary Method).

Model of quartz vein formation

We propose a model of quartz vein formation associated with fluid advection from host rocks and silica precipitation in a crack (Supplementary Method). An isolated disk-shaped crack exists at the center of a spherical host-rock reservoir of radius R meters (Fig. 2e). Pore fluids in the host rock are assumed to be always saturated with quartz at constant temperature and lithostatic pressure due to the pressure dissolution or free surface dissolution of sandstone²². At the time of an earthquake, the crack is opened, which causes a fluid pressure drop in the crack. The difference in fluid pressure between the host rock and the crack ($\Delta P = P_{\text{host}} - P_{\text{crack}}$) induces fluid advection from the host rock into the crack and silica precipitation in the crack. The two sides of the circular crack walls are the input paths of fluid from the host rock into the crack, whereas fluid flows radially through the crack for a distance equal to the radius. Based on the quartz vein textures (Figs. 2c,d), we consider silica precipitation as quartz overgrowth on pre-existing surfaces, governed by the kinetic equation of quartz overgrowth³³. We can define two kinds of fluid volume associated with quartz vein formation: (1) the fluid volume required for sufficient silica precipitation to seal a crack completely, which depends on the pressure drop and the kinetics of silica precipitation and (2) the fluid volume of the reservoir that supplies SiO_2 -supersaturated fluid by advection, which follows Darcy's law. We solve for the unique sealing time (t_s) simultaneously by iterating with the constraint that the two fluid volumes are equal (Supplementary Method).

In examining the formation of extensional cracks, we consider the realistic conditions around the Nobeoka Thrust (Supplementary Note). The initial pore fluid pressure and temperature of the extensional crack are set to 260 MPa and 250 °C, respectively, which are equivalent to the lithostatic conditions at a depth of 10 km on the Nobeoka Thrust (Fig. 3). The vein-forming fluids around the Nobeoka Thrust are considered to have neutral pH²² and low salinity²⁷, and we assume a constant SiO_2 concentration in the fluid in the host rock ($C_{\text{SiO}_2} = 6.0 \times 10^2 \text{ mg/kg(H}_2\text{O)}$), which is taken from the solubility of quartz in pure water at 250 °C and 260 MPa (Fig. 3)³⁴. The SiO_2 concentration in the fluid in the host rock (C_{SiO_2}) is $6.0 \times 10^2 \text{ mg/kg(H}_2\text{O)}$ as a result of pure water saturated via quartz at 250 °C and 260 MPa (Fig. 3)³⁴. As a typical example, we consider a crack with aperture width $w_v = 5.2 \times 10^1 \mu\text{m}$ and length $l_v = 7.4 \times 10^0 \text{ cm}$ (diameter), which are the geometric mean values of each parameter for extensional veins along the Nobeoka Thrust (Figs. 2a,b). We use a host-rock permeability of $1.0 \times 10^{-19} \text{ m}^2$, which is the average of previous measurements using a triaxial pressure apparatus (1×10^{-20} to $1 \times 10^{-18} \text{ m}^2$)³⁵. The porosity of the host rock ranges from 3% to 10%, as measured by geophysical wireline logs across the

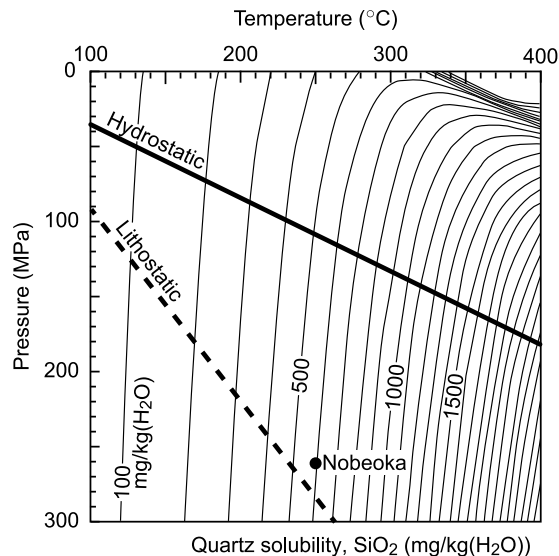


Figure 3. *P*-*T* diagram of quartz solubility with the conditions of the Nobeoka Thrust. Quartz solubility (SiO_2) is $6.0 \times 10^2 \text{ mg/kg(H}_2\text{O)}$ at a temperature of 250°C and a fluid pressure of 260 MPa in the host rock along the Nobeoka Thrust (black circle). Quartz solubility gradients are indicated by thin solid lines in units of $\text{mg/kg(H}_2\text{O)}$. The fluctuation between lithostatic (broken bold line) and hydrostatic (solid bold line) fluid pressure in the model of this study occurs at a temperature gradient of 20°C/km .

Nobeoka Thrust²³. In this study, we use a minimum porosity of 3% for most of the calculations, and we show that porosity has a minor influence on estimates of sealing time. The porosity and permeability of the host rock are set to be constant during crack sealing because the volume of quartz required to seal a crack is much smaller than that of the fluid reservoir in the host rock.

Results

When increasing ΔP from 0.1 to 160 MPa, so that the pore fluid pressure in the crack decreases from lithostatic to hydrostatic (Fig. 3), the degree of supersaturation in the crack ($C_{\text{SiO}_2}/C_{\text{SiO}_2, \text{Qtz, eq}} - 1$) increases from 7.1×10^{-5} to 1.9×10^{-1} , and the time taken for complete sealing of a crack becomes much shorter: for a typical crack, with $w_v = 5.2 \times 10^1 \mu\text{m}$ and $l_v = 7.4 \times 10^0 \text{ cm}$, the time decreases from 3.1×10^6 years (3.1 My) to 7.3×10^{-2} years (27 days) (Fig. 4a), where the reservoir size falls into the radius range $R = 4.9 \times 10^0$ to $3.9 \times 10^{-1} \text{ m}$ (Fig. 4b). While passing through the crack, the silica concentration (C_{SiO_2}) decreases to a level close to the solubility of quartz at each P_{crack} . Accordingly, the difference in SiO_2 concentration between the input and output fluid, which corresponds to the amount of silica precipitation, increases from $4.2 \times 10^{-2} \text{ mg/kg(H}_2\text{O)}$ at $\Delta P = 0.1 \text{ MPa}$ to $9.4 \times 10^1 \text{ mg/kg(H}_2\text{O)}$ at $\Delta P = 160 \text{ MPa}$ (Fig. 4b). In this ΔP range (0.1–160 MPa) at $T = 250^\circ\text{C}$, the sealing time (t_y) in years can be expressed as a logarithmic–linear function:

$$\log t_y = -2.4 \log \Delta P + 4.1. \quad (1)$$

This relationship shifts in parallel with any change in crack size except under certain conditions; e.g., when the sealing time of a crack of one-tenth the geometric mean length (i.e., $l_v = 7.4 \times 10^{-1} \text{ cm}$) becomes similar to that of a mean-length crack with increasing ΔP (Fig. 4a). In a smaller crack, the residence time of fluid in the crack is too short to precipitate all of the supersaturated SiO_2 . Thus, the difference in SiO_2 concentration between the input and output fluids in a smaller crack is smaller than that in a mean-sized crack at higher ΔP (Fig. 4b).

Given the mechanical properties of subduction megathrusts and the orientations of micro-fault systems (quartz veins), fluid pressure generated by extensional cracks can drop by up to 10% of lithostatic pressure ($\Delta P < \sim 25 \text{ MPa}$) during an earthquake³⁶. In addition, assuming a rock tensile strength of 10 MPa, cracks remain open in the range $\Delta P = 0$ –10 MPa. Hence, an appropriate range of ΔP for the formation of extensional quartz veins at around the Nobeoka Thrust is 10–25 MPa, for which the sealing time of a geometric mean size crack is 6.6×10^0 – 5.6×10^1 years (Fig. 4a). In this case, the radius of a spherical reservoir is 7.5×10^{-1} – $1.0 \times 10^0 \text{ m}$ (Fig. 4b). The sealing time depends on the conditions of the crack and the host rock. The sealing time of a crack of one-tenth the geometric mean length (i.e., $l_v = 7.4 \times 10^{-1} \text{ cm}$) ranges from 1.4×10^0 to 1.2×10^1 years at $\Delta P = 10$ –25 MPa (Fig. 4a). In the case of higher porosity (10%) and permeability ($1 \times 10^{-18} \text{ m}^2$), the sealing time of a geometric mean size crack is 4.4×10^{-1} – 3.8×10^0 years, while in the case of lower porosity (3%) and permeability ($1 \times 10^{-20} \text{ m}^2$) the sealing time is between 6.6×10^1 years and 5.6×10^2 years at $\Delta P = 10$ –25 MPa (Fig. 4a).

In addition to advection, diffusion could contribute to silica transport during vein formation. We calculated the sealing time for a model of vein growth via diffusive silica transport in pore fluids at $\Delta P = 0.1$ –160 MPa, following ref.³⁷ (Fig. 4a) (Supplementary Method). The driving force of silica transport in the diffusion model is the difference between the quartz solubility of the host rock and that of the cracks, and parameters such as ΔP are set to the same values as in the model of this study. The sealing time of a crack by diffusive transport of silica is slower

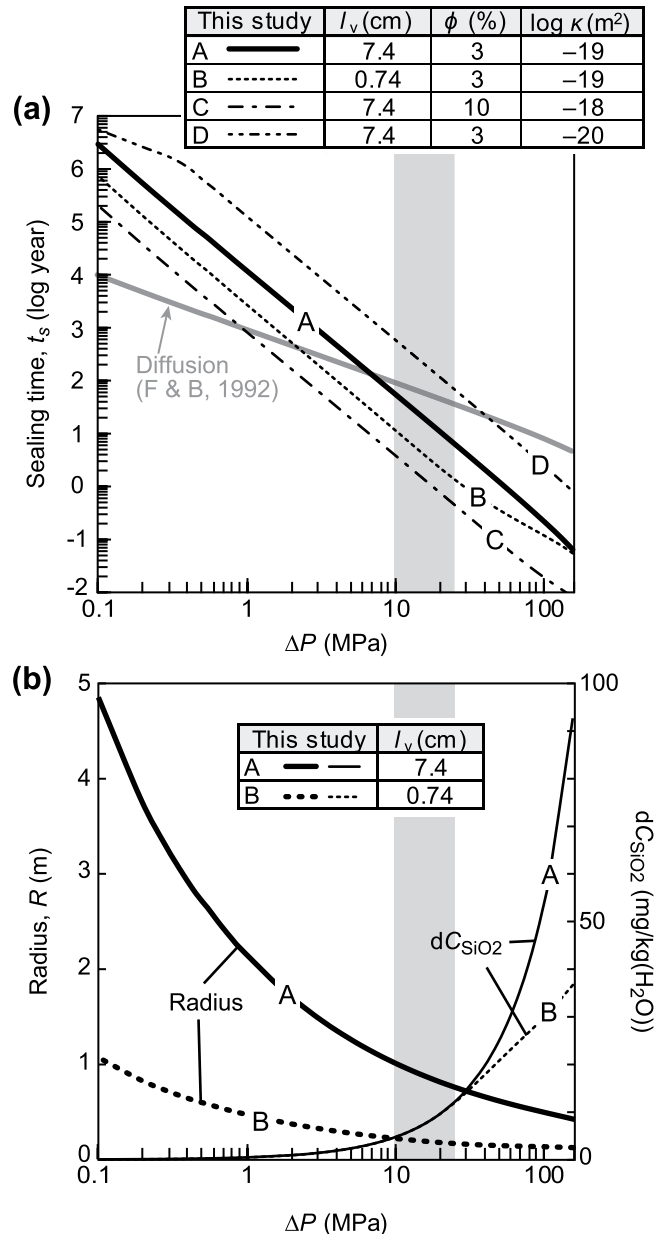


Figure 4. Crack sealing time and conditions. **(a)** Sealing times of extensional quartz veins calculated using our model (black lines, A–D) and a diffusion model (grey line)³⁷. **(b)** Reservoir radius (bold lines) and differences in fluid SiO₂ concentrations (thin lines). Fluid pressure drop (ΔP) is from 0.1 to 160 MPa. ‘A’ (solid black line) is a basic model comprising a geometric mean crack of aperture width ($w_v = 5.2 \times 10^1 \mu\text{m}$) and length ($l_v = 7.4 \times 10^0 \text{cm}$) in a host rock of porosity ($\phi = 3\%$) and permeability ($\kappa = 1 \times 10^{-19} \text{m}^2$). ‘B’ (dotted line) is a model comprising the reference size of a logarithmic–non-linear function ($l_v = 7.4 \times 10^{-1} \text{cm}$). The sealing time of a geometric mean size crack depending on porosity and permeability, is in the range between C ($\phi = 10\%$, $\kappa = 1 \times 10^{-18} \text{m}^2$) (chain line) and D ($\phi = 3\%$, $\kappa = 1 \times 10^{-20} \text{m}^2$) (double-dot chain line). Grey zone indicates the realistic range of fluid pressure drops along the Nobeoka Thrust ($\Delta P = 10$ – 25 MPa).

than the time estimated for our model under higher ΔP (Fig. 4a), but faster than our model under lower ΔP (< 8 MPa). In the possible range of fluid pressure drops along the Nobeoka Thrust ($\Delta P = 10$ – 25 MPa), the sealing time in the model of this study is 10^1 – 10^2 times faster than in the diffusive model (Fig. 4a). This implies that fluid advection is the dominant transport mechanism during extensional quartz vein formation along the Nobeoka Thrust, even if both processes occur there.

Crack volume is one of the critical factors for controlling the sealing time (Fig. 5). At $\Delta P = 25$ MPa, doubling the crack aperture or crack length increases the sealing time by a factor of two or four, respectively. We roughly estimated the presence probability of each volume of vein (0%–3%) by 225 all possible combinations of aperture width (Fig. 2a) and length (Fig. 2b). Figure 5 shows that most extensional veins in the Nobeoka Thrust seal within a period on the order of 1×10^0 – 1×10^1 years at $\Delta P = 25$ MPa (Fig. 5a) and on the order of 1×10^1 – 1×10^2 years

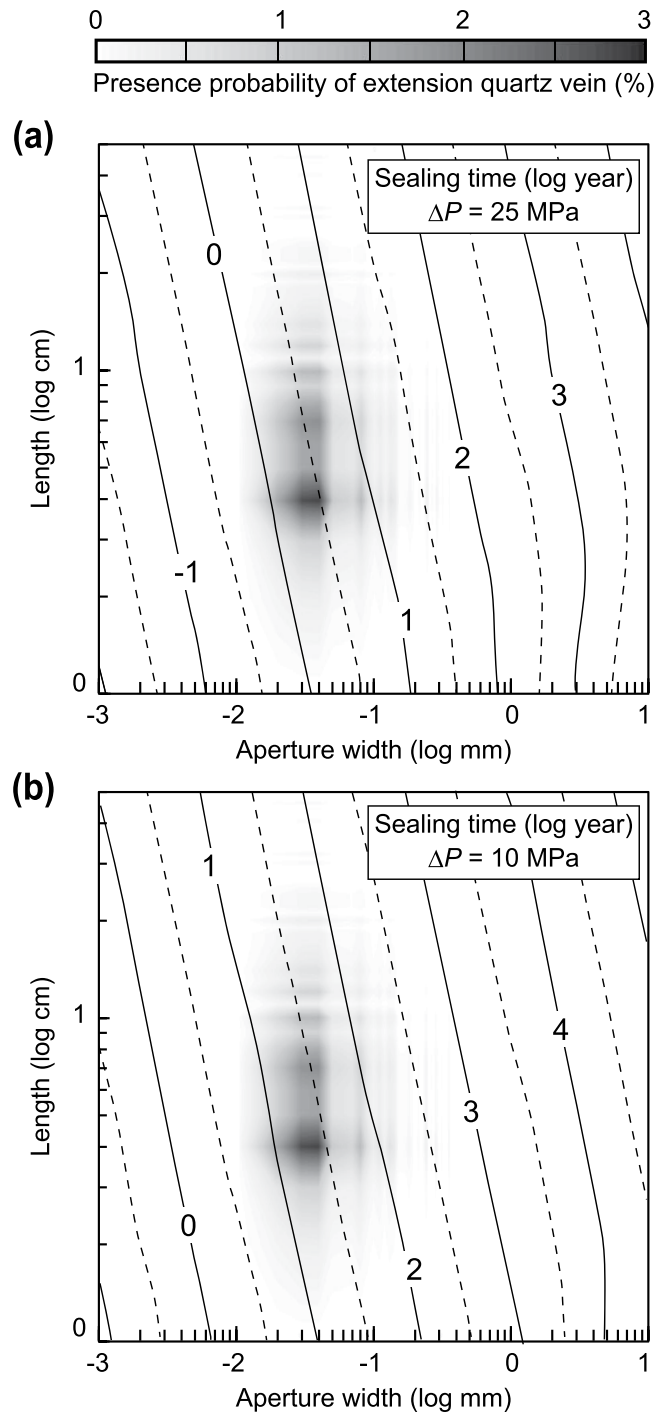


Figure 5. Probable sealing time of extensional quartz veins along the Nobeoka Thrust as a function of length and width of a crack. The difference in fluid pressure between the host rock and the crack (ΔP) is 25 MPa (a) and 10 MPa (b).

at $\Delta P = 10$ MPa (Fig. 5b). Thus, in the expected range of $\Delta P = 10$ –25 MPa, extensional cracks along the Nobeoka Thrust are sealed at timescales on the order of 1×10^0 – 1×10^2 years.

We clarify the effects of silica precipitation on the evolution of hydrological properties of an accretionary wedge. Because it is impossible to know the exact number of cracks generated during a single earthquake, we define a relative porosity index ($\Omega_t = 0$ –1) determined by the presence probability of each volume of veins with a cumulative number index of sealed crack ($\omega_t = 0$ –1), which is a rate between a cumulative number of completely sealed crack and total number of possible length-aperture width combinations obtained in this study (Supplementary Method). We assume that all cracks are opened ($\Omega_t = 1$, $\omega_t = 0$) at the time of earthquake rupture ($t = 0$) to show the range of duration of the porosity recovery period, and then Ω_t will decrease toward zero and ω_t will increase toward one by silica precipitation, respectively (Supplementary Method). This calculation does

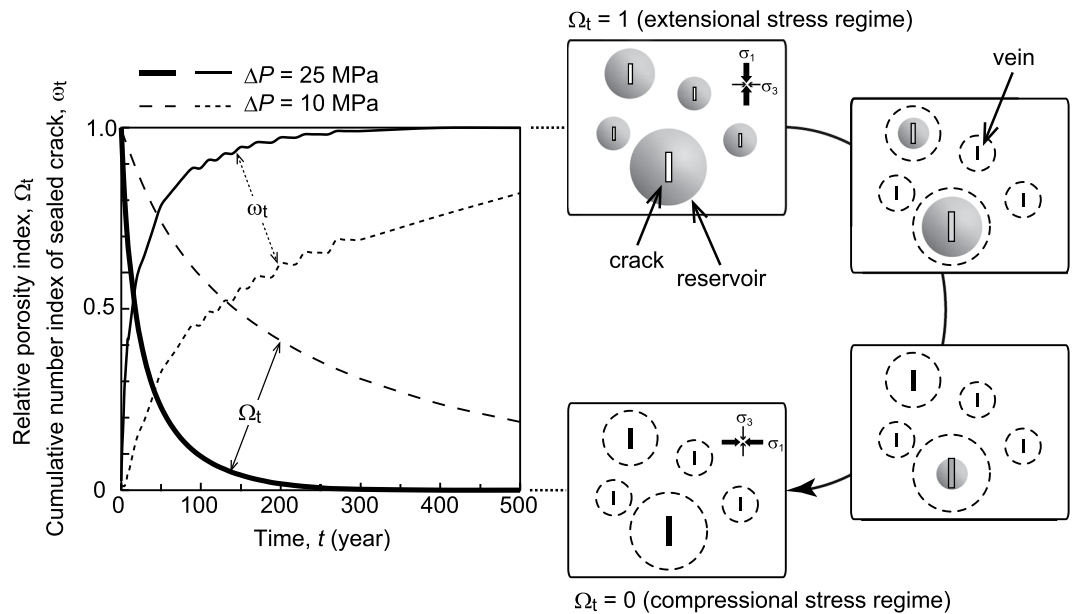


Figure 6. Temporal evaluation of relative porosity index and cumulative number index of sealed crack with conceptual image of crack sealing process. Relative porosity index (Ω_t) and cumulative number index of sealed crack (ω_t) at $\Delta P = 25$ MPa (solid lines) and 10 MPa (broken lines).

not consider the porosity of the host rock. Figure 6 shows that the relative crack porosity at $\Delta P = 25$ MPa could recover by 89% ($\Omega_t = 0.1$) to >99% ($\Omega_t < 0.01$) within 9×10^1 – 3×10^2 years, respectively. The cumulative frequency of complete sealed crack number is 89% within 90 years (Fig. 6). At $\Delta P = 10$ MPa, the relative porosity could recover by 38% ($\Omega_t = 0.62$) to 66% ($\Omega_t = 0.34$) within 9×10^1 – 3×10^2 years, respectively (Fig. 6), and 90% ($\Omega_t = 0.10$) within 8×10^2 years. The cumulative frequency of complete sealed crack number is 45% within 9×10^1 years, which is almost half of that at $\Delta P = 25$ MPa (Fig. 6).

Discussion

The sealing time of a crack depends on various factors, including porosity and permeability in the host rock, and fluid composition. For the area around the Nobeoka Thrust, estimates of sealing time are more strongly influenced by the permeability of the host rocks than the porosity. An increase in host-rock porosity from 3% to 10% reduces the sealing time by ~30% (Fig. 4a), and an increase in permeability from 1×10^{-18} m² to 1×10^{-20} m² results in a longer sealing time from 6.6×10^{-1} to 6.6×10^1 years (Fig. 4a). Several models of vein formation have been proposed, based on the diffusive transport of silica and pressure dissolution in the host rock^{12,18}. These studies also describe porosity reduction around the fault, but their model considered smaller cracks and lower ΔP than in the present study. The dominant transport mechanism contributing to quartz vein formation is diffusion at lower ΔP and advection at higher ΔP (Fig. 4a). The ΔP value that marks the transition in transport mechanism becomes lower with increasing permeability and porosity (Fig. 4a). Accordingly, the conditions (T , P , ΔP , vein size, host rock properties) inferred for the extensional quartz veins around the Nobeoka Thrust indicate that advection was the dominant transport mechanism during quartz vein formation.

The salinity and pH of a fluid affect quartz solubility³⁴ and the rate of quartz dissolution–precipitation³⁸. For example, at $\Delta P = \sim 160$ MPa, quartz solubility in seawater is $\sim 1.6 \times 10^1$ mg/kg(H₂O) lower than in pure water³⁴ (Supplementary Note) and the rate of quartz dissolution in seawater is about one order higher than that in pure water³⁸. Therefore, the sealing time of extensional quartz veins that formed from fluids with compositions similar to those that contributed to vein formation around the Nobeoka Thrust (i.e., neutral pH²² and salinity similar to or less than seawater²⁷) could be slightly shorter than that estimated in this study based on an assumption of pure water.

In natural systems, extensional quartz veins may occur in clusters, where the fluid catchments of neighboring cracks overlap with each other. Here we compare the sealing time of two simple systems, both of which contain the same volume of open cracks (1.0×10^{-7} m²). One system comprises a single crack ($w_v = 1.0 \times 10^2$ μ m, $V_{\text{crack}} = 1.0 \times 10^{-6}$ m²) and the other a cluster of 100 thin cracks of the same size ($w_v = 1.0 \times 10^0$ μ m, $V_{\text{crack}} = 1.0 \times 10^{-8}$ m² for each crack). At $\Delta P = 25$ MPa, the sealing time of the cluster (2.1×10^0 years) is $\sim 10^2$ times faster than that of the single crack (2.1×10^2 years) because of the larger surface area for quartz precipitation (Supplementary Eq. 1). However, it is not always clear whether all veins in a cluster formed during the same event. Further analyses of natural occurrences of vein clusters and the development of models will be required to enable more accurate estimates of sealing time.

The recurrence intervals of subduction thrust earthquakes^{39–42} are generally shorter than those of inland earthquakes^{43–46}. Since the Nobeoka Thrust is a good analogue of the seismogenic splay faults observed in the Nankai Trough⁴⁷, we provide quantitative constraints to link silica precipitation with the recurrence of subduction

thrust earthquakes in the Nankai Trough. At a depth of 10 km, comparable to the deeper part of the modern megasplay fault in the Nankai Trough^{19,48}, the sealing time of the extensional cracks smaller than $w_v = 5.2 \times 10^1 \mu\text{m} \times l_v = 7.4 \times 10^0 \text{cm}$ ($\sim 5.6 \times 10^1$ years; Fig. 4), is similar to the expected duration of the extensional stress regime in the Nankai Trough ($\sim 3 \times 10^1$ years)^{1,2}. For complete sealing of larger cracks, silica precipitation should continue in the openings of larger cracks even after the stress regime changes to compression, because our field studies revealed no evidence for multiple crack–seal events in any single extensional quartz vein (Fig. 2d). Considering that the rate of quartz overgrowth depends on the crystallographic orientations of seed crystals on crack walls, crack sealing in large open cavities is heterogeneous, and quartz crystals grow quickly from both side-walls to impinge on one another⁴⁹; thus, collapse of the cracks is prevented, even after a change in stress regime.

Under the conditions expected along the Nobeoka Thrust, almost all extensional quartz veins form within $\sim 1 \times 10^2$ years (Fig. 5), and the relative crack porosity at $\Delta P = 25$ MPa could recover by >99% within $\sim 3 \times 10^2$ years (Fig. 6) known recurrence interval of megathrust events in the Nankai Trough, respectively^{1,2}. This result suggests that when megathrust earthquakes form extensional cracks in the accretionary wedge, the porosity is nearly recovered by silica precipitation within the aseismic interval, regardless of crack size. Figure 6 also suggests that a larger pressure drop facilitates a much more drastic porosity recovery. A spherical reservoir with a radius of 7.5×10^{-1} – 1.0×10^0 m, as required to seal a crack of mean size in the model of this study (Fig. 4b), is greater than the vein spacing observed in thin sections, suggesting that the set of quartz veins observed in our field study might not have formed from a single event. However, with the assumption that cracks with all possible combinations of length and aperture width are opened at the time of earthquake rupture (Fig. 6), our model is applicable to any number of crack openings, because the relative porosity is the ratio of the number of sealed cracks to the number of open cracks (Supplementary Method).

A decrease in sandstone porosity leads to the permeability decrease as recognized in various hydrostatic compression tests⁵⁰, which may result in increased fluid pressure due to sealing of flow paths and supplying of fluid from deeper parts²², thereby leading to an increased probability of earthquake occurrence^{36,51}. The fault-valve model⁸ describes a cycle wherein instantaneous permeability rises and fluid pressure drops at the time of an earthquake; these quantities then decrease and rise again, respectively, as the fault approaches the next earthquake. Therefore, the geochemical evolution of accretionary wedge porosity, as proposed in this study, relates to the evolution of permeability and fluid pressure in the earthquake cycle. Decreasing porosity enhances the build-up of pore fluid pressure because the fluid is supplied by flowing or percolating in the bulk and along faults or décollement during both pre- and post-seismic²⁷. Pore pressure builds-up with increasing the number of closed extension cracks, which may not be in one-to-one relationship, and its timescale is similar to that of crack sealing. The high porosity generated at the time of an earthquake under extensional stress is followed by a rapid decrease just after the earthquake. During the low porosity regime, when the likelihood of the next earthquake is already high, porosity still decrease due to silica precipitation in larger cracks when the pressure difference between the host rock and cracks is maintained before an earthquake (Fig. 6). We conclude that silica precipitation generates subcritical conditions for earthquakes (i.e., lower porosity, lower permeability, higher fluid pressure) and thus controls earthquake recurrence intervals in seismogenic zones. The next megathrust earthquake may occur when these conditions reach critical values.

Data availability. The datasets generated during the current study are available from the corresponding author on reasonable request.

References

- Dieterich, J. A constitutive law for rate of earthquake production and its application to earthquake clustering. *J. Geophys. Res.* **99**, 2601–2618 (1994).
- Hyodo, M., Hori, T., Ando, K. & Baba, T. The possibility of deeper or shallower extent of the source area of Nankai Trough earthquakes based on the 1707 Hōei tsunami heights along the Pacific and Seto Inland Sea coasts, southwest Japan. *Earth Planets Space* **66**, 123 (2014).
- Ikuta, R., Mitsui, Y., Kurokawa, Y. & Ando, M. Evaluation of strain accumulation in global subduction zones from seismicity data. *Earth Planets Space* **67**, 192 (2015).
- Screaton, E. J. *et al.* Porosity loss within underthrust sediments of the Nankai accretionary complex: Implications for overpressures. *Geology* **30**, 19–22 (2002).
- Saffer, D. M. Pore pressure development and progressive dewatering in underthrust sediments at the Costa Rican subduction margin: Comparison with northern Barbados and Nankai. *J. Geophys. Res.* **108**, 2261 (2003).
- Tobin, H. J. & Saffer, D. M. Elevated fluid pressure and extreme mechanical weakness of a plate boundary thrust, Nankai Trough subduction zone. *Geology* **37**, 679–682 (2009).
- Tsuji, T., Kamei, R. & Pratt, R. G. Pore pressure distribution of a mega-splay fault system in the Nankai Trough subduction zone: Insight into up-dip extent of the seismogenic zone. *Earth Planet. Sci. Lett.* **396**, 165–178 (2014).
- Sibson, R. H. Implications of fault-valve behavior for rupture nucleation and recurrence. *Tectonophysics* **18**, 1031–1042 (1992).
- Cox, S. F. Faulting processes at high fluid pressures: An example of fault-valve behavior from the Wattle Gully fault, Victoria, Australia. *J. Geophys. Res.* **100**, 12841–12859 (1995).
- Ujiiie, K., Yamaguchi, A., Kimura, G. & Toh, S. Fluidization of granular material in a subduction thrust at seismogenic depths. *Earth Planet. Sci. Lett.* **259**, 307–318 (2007).
- Faber, C. *et al.* Silica gel in a fault slip surface. *Field evidence for palaeo-earthquakes?* *J. Struct. Geol.* **69**, 108–121 (2014).
- Fisher, D. M. & Brantley, S. L. The role of silica redistribution in the evolution of slip instabilities along subduction interfaces: Constraints from the Kodiak accretionary complex, Alaska. *J. Struct. Geol.* **69**, 395–414 (2014).
- Weatherley, D. K. & Henley, R. W. Flash vaporization during earthquakes evidenced by gold deposits. *Nature Geoscience* **6**, 294–298 (2013).
- Di Toro, G. *et al.* Fault lubrication during earthquakes. *Nature* **471**, 494–498 (2011).
- Kirkpatrick, J. D. *et al.* Silica gel formation during fault slip: Evidence from the rock record. *Geology* **41**, 1015–1018 (2013).
- Fagereng, Å. & den Hartog, S. A. M. Subduction megathrust creep governed by pressure solution and frictional–viscous flow. *Nature Geoscience* **10**, 51–57 (2017).

17. Audet, P. & Bürgmann, R. Possible control of subduction zone slow-earthquake periodicity by silica enrichment. *Nature* **510**, 389–392 (2014).
18. Renard, F., Jean-Pierre, G. & Bjørn, J. Kinetics of crack-sealing, intergranular pressure solution, and compaction around active faults. *J. Struct. Geol.* **22**, 1395–1407 (2000).
19. Kondo, H. *et al.* Deformation and fluid flow of a major out-of-sequence thrust located at seismogenic depth in an accretionary complex: Nobeoka Thrust in the Shimanto Belt, Kyushu, Japan. *Tectonics* **24**, 1–16 (2005).
20. Okamoto, A., Kikuchi, T. & Tsuchiya, N. Mineral distribution within polyminerale veins in the Sanbagawa belt, Japan: implications for mass transfer during vein formation. *Contrib. Min. Petr.* **156**, 323–336 (2008).
21. Otsubo, M. *et al.* Variation of stress and pore fluid pressure using vein orientation along seismogenic megasplay fault - example of Nobeoka Thrust, southwestern Japan. *Island Arc* **25**, 421–432 (2016).
22. Yamaguchi, A., Cox, S. F., Kimura, G. & Okamoto, S. Dynamic changes in fluid redox state associated with episodic fault rupture along a megasplay fault in a subduction zone. *Earth Planet. Sci. Lett.* **302**, 369–377 (2011).
23. Hamahashi, M. *et al.* Multiple damage zone structure of an exhumed seismogenic megasplay fault in a subduction zone - a study from the Nobeoka Thrust Drilling Project. *Earth Planets Space* **67**, 30 (2015).
24. Kawasaki, R. *et al.* Temporal stress variations along a seismogenic megasplay fault in the subduction zone: an example from the Nobeoka Thrust, southwestern Japan. *Island Arc* **26**, e12193 (2017).
25. Hasegawa, A. *et al.* Change in stress field after the 2011 great Tohoku-Oki earthquake. *Earth Planet. Sci. Lett.* **355–356**, 231–243 (2012).
26. Hashimoto, Y. *et al.* Changes in paleostress state along a subduction zone preserved in an on-land accretionary complex, the Yokonami mélange in the Cretaceous Shimanto Belt, Kochi, southwest Japan. *Tectonics* **33**, 2045–2058 (2014).
27. Raimbourg, H. *et al.* Fluid circulation in the depths of accretionary prisms: an example of the Shimanto Belt, Kyushu, Japan. *Tectonophysics* **655**, 161–176 (2015).
28. Hara, H. & Kimura, K. Metamorphic and cooling history of the Shimanto accretionary complex, Kyushu, Southwest Japan: Implications for the timing of out-of-sequence thrusting. *Island Arc* **17**, 546–559 (2008).
29. Raimbourg, H., Shibata, T., Yamaguchi, A., Yamaguchi, H. & Kimura, G. Horizontal shortening versus vertical loading in accretionary prisms. *Geochem. Geophys. Geosyst.* **10**, Q04007 (2009).
30. Yamaji, A., Sato, K. & Tonai, S. Stochastic modeling for the stress inversion of vein orientations: Paleostress analysis of Pliocene epithermal veins in southwestern Kyushu, Japan. *J. Struct. Geol.* **32**, 1137–1146 (2010).
31. Collettini, C. & Sibson, R. H. Normal faults, normal friction. *Geology* **29**, 927–930 (2001).
32. Ramsay, J. G. The crack-seal mechanism of rock deformation. *Nature* **284**, 135–139 (1980).
33. Rimstidt, J. D. & Barnes, H. L. The kinetics of silica-water reactions. *Geochim. Cosmochim. Acta* **44**, 1683–1699 (1980).
34. Akinfev, N. N. & Diamond, L. W. A simple predictive model of quartz solubility in water-salt-CO₂ systems at temperatures up to 1000 °C and pressures up to 1000 MPa. *Geochim. Cosmochim. Acta* **73**, 1597–1608 (2009).
35. Kato, A. *et al.* Permeability structure around an ancient exhumed subduction-zone fault. *Geophys. Res. Lett.* **31**, L06602 (2004).
36. Sibson, R. H. Stress switching in subduction forearcs: Implications for overpressure containment and strength cycling on megathrusts. *Tectonophysics* **600**, 142–152 (2013).
37. Fisher, D. M. & Brantley, S. L. Model of quartz overgrowth and vein formation: deformation and episodic fluid flow in an ancient subduction zone. *J. Geophys. Res.* **97**, 20043–20061 (1992).
38. Dove, P. M. The dissolution kinetics of quartz in sodium chloride solutions at 25 °C to 300 °C. *Am. J. Sci.* **294**, 665–712 (1994).
39. Ito, T., Yoshioka, S. & Miyazaki, S. Interplate coupling in southwest Japan deduced from inversion analysis of GPS data. *Phys. Earth Planet. Int.* **115**, 17–34 (1999).
40. Nanayama, F. *et al.* Nine unusually large tsunami deposits from the past 4000 years at Kiritappu marsh along the southern Kuril Trench. *Sediment. Geol.* **200**, 275–294 (2007).
41. Nakata, R., Miyazaki, S., Hyodo, M. & Hori, T. Reproducibility of spatial and temporal distribution of aseismic slips in Hyuga-nada of southwest Japan. *Mar. Geophys. Res.* **35**, 311–317 (2014).
42. Perfettini, H. & Avouac, J. P. The seismic cycle in the area of the 2011 Mw9.0 Tohoku-Oki earthquake. *J. Geophys. Res.* **119**, 4469–4515 (2014).
43. Wells, D. L. & Coppersmith, K. J. New empirical relationships among magnitude, rupture length, rupture width, rupture area, and surface displacement. *Bull. Seism. Soc. Am.* **84**, 974–1002 (1994).
44. Takeuchi, A. & Ongirad, H. Recurrence interval of big earthquakes along the Atotsugawa fault system, central Japan: Results of seismo-geological survey. *Geophys. Res. Lett.* **30**, 8011 (2003).
45. Sato, H. *et al.* Holocene crustal movement along the coast of western Kobe and the 1995 Kobe Earthquake, Japan. *Quat. Sci. Rev.* **22**, 891–897 (2003).
46. Hornblow, S., Quigley, M., Nicol, A., Van Dissen, R. & Wang, N. Paleoseismology of the 2010 M_w 7.1 Darfield (Canterbury) earthquake source, Greendale Fault, New Zealand. *Tectonophysics* **637**, 178–190 (2014).
47. Kimura, G. *et al.* Hanging wall deformation of a seismogenic megasplay fault in an accretionary prism: The Nobeoka Thrust in southwestern Japan. *J. Struct. Geol.* **52**, 136–147 (2013).
48. Hamahashi, M. *et al.* Contrasts in physical properties between the hanging wall and footwall of an exhumed seismogenic megasplay fault in a subduction zone - An example from the Nobeoka Thrust Drilling Project. *Geochem. Geophys. Geosyst.* **14**, 5354–70 (2013).
49. Okamoto, A. & Sekine, K. Textures of syntaxial quartz veins synthesized by hydrothermal experiments. *J. Struct. Geol.* **33**, 1764–1775 (2011).
50. Bernabe, Y., Mok, U. & Evans, B. Permeability-porosity Relationships in Rocks Subjected to Various Evolution Processes. *Pure Appl. Geophys.* **160**, 937–960 (2003).
51. Peacock, S. M., Christensen, N. I., Bostock, M. G. & Audet, P. High pore pressures and porosity at 35 km depth in the Cascadia subduction zone. *Geology* **39**, 471–474 (2011).
52. Murata, A. Duplexes and low-angle nappe structures of the Shimanto Terrane, southwest Japan. *Mem. Geol. Soc. Japan* **50**, 147–158 (1998).
53. A Illustrator, <http://www.adobe.com/products/illustrator.html> (2016).

Acknowledgements

The authors would like to thank A. Yamaguchi, M. Hamahashi and W. Tanikawa for their constructive comments on the calculation conditions and the model concepts. A.O. received further support through JSPS KAKENHI Grant Number 26287132.

Author Contributions

M.O. conceived the initial concept and H.S. and A.O. expanded the model. M.O. observed the extensional quartz veins and summarized parameters of the Nobeoka Thrust. H.S. calculated the crack sealing timescales. All authors wrote the manuscript and composed the figures.

Additional Information

Supplementary information accompanies this paper at <https://doi.org/10.1038/s41598-017-13597-5>.

Competing Interests: The authors declare that they have no competing interests.

Publisher's note: Springer Nature remains neutral with regard to jurisdictional claims in published maps and institutional affiliations.



Open Access This article is licensed under a Creative Commons Attribution 4.0 International License, which permits use, sharing, adaptation, distribution and reproduction in any medium or format, as long as you give appropriate credit to the original author(s) and the source, provide a link to the Creative Commons license, and indicate if changes were made. The images or other third party material in this article are included in the article's Creative Commons license, unless indicated otherwise in a credit line to the material. If material is not included in the article's Creative Commons license and your intended use is not permitted by statutory regulation or exceeds the permitted use, you will need to obtain permission directly from the copyright holder. To view a copy of this license, visit <http://creativecommons.org/licenses/by/4.0/>.

© The Author(s) 2017